GSI

GSI - 82 - 34
PREPRINT

DECAY STUDIES OF NEUTRON - RICH PRODUCTS FROM ^{76}Ge - INDUCED MULTINUCLEON TRANSFER REACTIONS INCLUDING THE NEW ISOTOPES ^{62}Mn, ^{63}Fe AND $^{71,72,73}Cu$

E. Runte, W.-D. Schmidt-Ott, P. Tidemand-Petersson, R. Kirchner, O. Klepper, W. Kurcewicz, E. Roeckl, N. Kaffrell, P. Peuser, K. Rykaczewski, M. Bernas, P. Dessagne, and M. Langevin

November 1982

Gesellschaft für Schwerionenforschung mbH
Planckstr. 1 · Postfach 110541 · D-6100 Darmstadt 11 · Germany

DECAY STUDIES OF NEUTRON-RICH PRODUCTS FROM ^{76}Ge-INDUCED MULTINUCLEON TRANSFER REACTIONS INCLUDING THE NEW ISOTOPES ^{62}Mn, ^{63}Fe AND ^{71,72,73}Cu

E. RUNTE, W.-D. SCHMIDT-OTT and P. TIDEMAND-PETERSSON
II. Physikalisches Institut, Universität Göttingen,
3400 Göttingen, Fed. Rep. of Germany
R. KIRCHNER, O. KLEPPER, W. KURCEWICZ+ and E. ROECKL
GSI Darmstadt, 6100 Darmstadt, Fed. Rep. of Germany
N. KAFFRELL and P. PEUSER
Institut für Kernchemie, Universität Mainz, 6500 Mainz,
Fed. Rep. of Germany
K. RYKACZEWSKI++
Instytut Fizyki Doswiadczalnej, Uniwersytet Warszawski,
00-681 Warsaw, Poland
and
M. BERNAS, P. DESSAGNE and M. LANGEVIN
Institut de Physique Nucléaire, BP n° 1, 91406 Orsay, France

RADIOACTIVITY ^{62}Mn, ^{63}Fe, ^{67}Ni, ^{71,72,73}Cu, ^{73,74}Zn [from W(^{76}Ge,X); E = 9 MeV/nucleon, mass separation]; measured E_γ, I_γ, $\beta\gamma$-, $\gamma\gamma$-coin, $T_{1/2}$; deduced log ft. ^{62}Fe, ^{63}Co, ^{71,72}Zn, ^{73,74}Ga deduced levels, J,π. Plastic scintillator, Ge(Li), Ge(i) detectors.

(Submitted for publication in Nucl. Phys. A)
(Göttingen-November 1982)

+ On leave of absence from Institute of Experimental Physics, Warsaw University, 00-681 Warsaw, Poland
++ Partially supported by Polish Ministry of Science, High Education and Technics under the contract MR.I.5.13.01

Abstract: By irradiating a ^{nat}W target with 9 MeV/u ^{76}Ge ions neutron-rich isotopes in the chromium-germanium region were produced. On-line mass-separated samples were investigated. The new isotopes ^{62}Mn, ^{71}Cu, ^{72}Cu and ^{73}Cu were identified and their half-lives measured to be 0.88(15), 19.5(16), 6.6(1) and 3.9(3) s, respectively. The half-life of ^{63}Fe, a nucleus which has previously been detected using particle-identification techniques, was measured to be 4.9(5) s. Decay schemes were derived in most cases. Additional spectroscopic information was obtained on the decays of ^{73}Zn and ^{74}Zn. We give evidence that the earlier reported γ-ray activity attributed to ^{67}Ni belongs to the decay of the ^{70}Cu isomers. At A = 67 we observed a new ß-ray activity of 21(1) s half-life which is here assigned to the decay of ^{67}Ni.

1. Introduction

The chart of the nuclides, as presently known [1], displays two extended areas of β^--decaying nuclei which have been studied as fission products. A new way to investigate other neutron-rich nuclei is provided by deep-inelastic reactions induced by energetic heavy ions. It has already been shown that such species were formed with yields large enough to allow their identification from their decay properties, using standard on-line mass-separator techniques [2]. Target-like products, situated above the heavy fission-product group, were generated in collisions of a ^{136}Xe beam on a ^{nat}W/Ta target.

Here we have investigated the neutron-rich nuclei located under the light products of the asymmetric fission. Although it has been rather inaccessible until now, spectroscopy in this region is bringing crucial information for nucleosynthesis calculations. The neutron-rich nuclides were obtained as projectile-like products from irradiation of a ^{nat}W target with ^{76}Ge ions. In analogy with our first application of the multinucleon transfer reaction [2] we have again concentrated on decay studies of nuclides, for which the mass-separated samples were sufficiently intense. In addition to known nuclides of the elements chromium through germanium with A = 56-75, we identified the decays of ^{62}Mn, ^{63}Fe and $^{71,72,73}Cu$, of which only ^{63}Fe was known from direct particle-identification measurements [3] to be bound.

2. Experimental techniques

The experiment was performed by bombarding a 23 mg/cm^2 ^{nat}W target with a 9 MeV/u ^{76}Ge beam of 4-15 particle·nA from the UNILAC accelerator at GSI. The reaction products were stopped in a 30 mg/cm^2 graphite catcher inside a FEBIAD-E ion source [4] of the on-line mass separator [5].

Two mass-separated beams of reaction products were collected simultaneously at movable-tape systems and transported to the measuring positions after preselected accumulation times. In each counting position two germanium detectors were arranged in 180^o geometry with a 0.5 mm thick (4π and 2π, respectively) plastic scintillator inbetween. Beta- and γ-ray activities were investigated by singles (including multispectrum analysis) and coincidence measurements. The coincidence resolving time was 1 μs. For the listmode data each event was tagged with time marks.

3. Experimental results and discussion

The region of the nuclear chart investigated in this work is shown in fig. 1. Observed nuclides are labelled with measured saturation activities of mass-separated samples; we have accentuated the new nuclides and the isotopes for which new decay data are obtained in this work. The properties of these isotopes will be presented in the following sections.

3.1 THE $^{62}Mn \longrightarrow {}^{62}Fe$ DECAY

A part of the ß-coincident γ-ray spectrum measured for mass 62 is given in fig. 2 showing some new transitions besides known γ-lines from the decays of ^{62}Fe and ^{62}Co [ref. [6]]. The assignment of the new activity to the ß-decay of ^{62}Mn is based on the agreement between the energy of 877 keV of the most intensive new γ-transition and the energy of the first 2^+ level in the nucleus ^{62}Fe, which was measured in $^{64}Ni(^{14}C,^{16}O)$ [ref. [7]] and $^{64}Ni(^{18}O,^{20}Ne)$ [ref. [8]] reactions to be 0.86(4) and 0.875(10) MeV, respectively. The decay curves of this 877 keV ground-state transition and of ß-rays (after correction for iron and cobalt ß-rays) yield half-lives which agree within a value of $T_{1/2}$ = 0.88(15) s. The other γ-lines were assigned to ^{62}Mn from a similar decay behaviour. The relative intensities of these 876.8(3), 942.1(4), 1299.0(4), 1457.4(5), 1815.0(6) and 2016.0(8) keV transitions are 100(10), 29(8), 28(9), 16(7), 23(8) and 11(6), respectively. The 834.5 keV transition, for which no assignment is made, has not been observed in earlier studies of mass-62 nuclei [6]; a relationship to the decay of ^{62}Mn is improbable, since no decrease in the count-rate was observed within the 4.2 s measuring-time interval.

The decay scheme of ^{62}Mn shown in fig. 3 was constructed on the basis of energy considerations and intensity balances. The levels at 1820, 2016 and 2176 keV may be interpreted as the 0^+, 2^+, 4^+ triplet of the two phonon excitation. Spins and parities of levels in fig. 3 were assigned tentatively considering the following arguments:

a) The 2016 keV level shows direct γ-decay into the ground state. We therefore assigned $I^\pi = 2^+$ to this state.
b) The levels at 1820 and 2176 keV, representing the 0^+ and the 4^+ members of the triplet, are both populated by γ-transitions from the 3634 keV state, which leads to the assumption of $I^\pi = 2^+$ for that highest identified level. As expected we observe no ground-state γ-transitions from the 0^+ and 4^+ states.
c) In contrast to the 2176 keV level, the 1820 keV state is not fed directly by ß-decay, nor is the 0^+ ground state, the latter result following from a comparison of the intensities of singles ß-rays and ß-coincident γ-rays; we propose therefore to assign 0^+ to the 1820 keV level, which leaves 4^+ as the only possibility for the 2176 keV state.

The $2^+ \longrightarrow 2^+$ transition between the 2016 keV state and the first excited state was not observed in the γ-ray spectrum.

The log ft values were deduced using ref. [9] and a Q_β-value of 10.3 MeV; the latter value represents an average (with a deviation of ±0.6 MeV) calculated from the mass-formula predictions of ref. [10]. Accordingly, ^{62}Mn decays by allowed ß-transitions into 2^+ and 4^+ levels [11] and has the ground-state spin and parity $I^\pi = 3^+$ in analogy with the even-A manganese isotopes with A = 54-60 [refs. [6,12]].

3.2 THE $^{63}Fe \longrightarrow {}^{63}Co$ DECAY

Guerrau et al. [3] first observed the neutron-rich nucleus ^{63}Fe by means of ΔE-E techniques irradiating ^{238}U with ^{40}Ar. We have studied decay properties of ^{63}Fe. A part of the ß-coincident γ-ray spectrum measured at A = 63 is shown in fig. 4. Three new γ-transitions with energies of 994.8(5), 1364.7(5) and 1427.5(5) keV can be identified as ground-state transitions from the three lowest lying excited states in ^{63}Co, known from $^{64}Ni(t,\alpha)$ [ref. [13]] and $^{64}Ni(d,{}^3He)$ [ref. [14]] reactions. The relative intensities of these γ-lines are 100(5), 37(6) and 46(6), respectively. The decay curve of the 995 keV γ-line gives the half-life 4.9(5) s for ^{63}Fe. From the reaction data of refs. [13,14] possible spin and parity assignments of the ground state and the first excited state of ^{63}Co are $7/2^-$ or $5/2^-$ and $1/2^-$ or $3/2^-$, respectively. For the ground state the value $I^\pi = 7/2^-$ is very probable considering the shell model prediction and the fact that all known odd-A cobalt isotopes [6] follow that prediction. Then we deduce $I^\pi = 3/2^-$ for the 995 keV level from the occurrence of the ß-coincident ground-state transition. The corresponding state is observed in the neighbouring cobalt isotopes and also predicted by the shell model as the first proton hole state above the ground state.

The resulting decay scheme of ^{63}Fe is given in fig. 5. The ground-state ß-feeding was calculated as described in sect. 3.1 to be 76(26)%. The Q_β-value of 6.66(6) MeV was taken from the mass excess of ^{63}Co [ref. [6]] and a recent Q-value measurement of the reaction $^{64}Ni({}^{14}C,{}^{15}O){}^{63}Fe$ [ref. [15]]. The deduced log ft values for ß-decays leading to the $3/2^-$ and $7/2^-$ states suggest an allowed character of these transitions and, hence, $I^\pi = 5/2^-$ for the ground state of ^{63}Fe. This is in accordance with the neighbouring N=37 isotones of nickel, zinc, germanium and probably selenium all having ground states with $I^\pi = 5/2^-$ [ref. [6]] as expected from shell-model considerations.

3.3 THE $^{67}Ni \longrightarrow {}^{67}Co$ DECAY

Studying the products from reactions induced by 14 MeV neutrons in ^{70}Zn, Taff, Koene and van Klinken [16] observed several unknown γ-lines, a part of which has unambiguously been identified to follow the decays of the two ^{70}Cu isomers. Further γ-rays with a half-life of 18(4) s have been attributed to the decay of ^{67}Ni. Reiter, Breunlich and Hille [17] remeasured the results of Taff et al. in a similar experiment using enriched ^{70}Zn targets and a fast neutron beam. They reported a 16(4) s ß- and γ-activity which they also assigned to the ^{67}Ni decay. Our present measurement is not in agreement with the results of both experiments. Using mass separated samples we observed the most intensive of the earlier reported 16 and 18 s γ-rays [16,17] with energies of 208.4, 708.2, 1072.2, 1654.1 and 1787.0 keV at mass 70 and reassign these to ^{70}Cu. In support of our results the 1072 keV γ-rays have also been seen as reaction γ-rays in the $^{70}Zn(n,n')$ process[6]. The half-life values of 16 and 18 s can be explained, if both isomeric states in ^{70}Cu with half-lives of 5 and 42 s, respectively, contribute to the ß- and γ-decays.

In our experiment no γ-ray activity was observed at A = 67 using a 49 s collection and counting time during a total measurement of 22 min. However, we have measured a short-lived ß-activity with a half-life of $T_{1/2}$ = 21(1) s. The decay curve is given in fig. 6. We have tentatively assigned this activity to ^{67}Ni. Half-life predictions for the lower-Z isobaric nuclide ^{67}Co (4 s ref. [18] and 1.9 s ref. [19]) are smaller by one order-of-magnitude than the experimental value. From the non observation of γ-ray activity we estimate the upper limit of 8% for γ-rays below 1.5 MeV. The predominant ß-decay directly to the ^{67}Cu ground state is in agreement with the expectation based on the probable ground-state spins and parities $1/2^-$ and $3/2^-$ of ^{67}Ni and ^{67}Cu [ref. [16]], respectively, whereas in the $^{67}Co \longrightarrow {}^{67}Ni$ decay the ß-feeding of the ground state in the final nucleus is very unlikely. This is, because $I^{\pi} = 7/2^-$ is observed for the ground states of all known odd-A Co isotopes in agreement with the shell model.

3.4 THE $^{71}Cu \longrightarrow {}^{71}Zn$ DECAY

The results of our studies on the decay of ^{71}Cu are presented in table 1. The spectrum in fig. 7 is composed of γ-activity following the decays of the two isomers of ^{71}Zn [ref. [6]] and an activity with significantly shorter half-life, which can be assigned to ^{71}Cu, because almost all new γ-lines fit into the level scheme of ^{71}Zn known from the $^{70}Zn(d,p)$ reaction [20] (see fig. 8) and are ß-coincident. The half-life is determined to be 19.5(9) s from the decays of the 129, 198 and 675 keV γ-rays.

Like in the other known odd-A copper nuclei, the ground-state spin and parity is expected to be $I^{\pi} = 3/2^-$, due to the 29th proton in the $p_{3/2}$ shell. In agreement with this prediction we observe ß-feeding of I=1/2 and I=5/2 levels in the final nucleus. The spin values in fig. 8 are taken from ref. [20] except that of the 1791 keV level, which results from the occurrence of ß-feeding to this state. Log ft values were not deduced, because the absolute ß-intensities were not measured in the mass-71 experiment, and thus the direct population of the ^{71}Zn ground state could not be evaluated. The relative ß-branches and total γ-transition intensities in fig. 8 are normalized to the intensity of the 129 keV γ-line. The more intensive 490 and 595 keV transitions, placed in the level scheme, were not used for normalization, since they belong to doublets in the γ-ray spectrum, as manifested by their decay curves. Their intensities result from the number of counts in the γ-lines after subtraction of components belonging to transitions in ^{71}Ga. The intensities of the 129 and the 198 keV transitions in fig. 8 are corrected for internal conversion using the tables of Rösel et al. [21] and assuming multipolarity E2.

3.5 THE $^{72}Cu \longrightarrow {}^{72}Zn$ DECAY

The γ-ray spectrum, recorded at A=72 and given in part in fig. 9, mainly contains radiation of a new activity and some known transitions from the decays of ^{72}Zn and ^{72}Ga [ref. [6]]. Most of the new γ-lines presented in table 2 can be placed into the level scheme of ^{72}Zn, which was known already from $^{70}Zn(t,p)$ reaction data [22]; the observed activity is hence assigned to the decay of ^{72}Cu. The strong transitions with energies of 652, 846, 1005, 1540 and 1658 keV and the β-ray activity determine the half-life of ^{72}Cu to be 6.6(1) s.

The decay scheme in fig. 10 was constructed using intensity and energy fits and informations from γγ-coincidences. We have introduced three additional states at 2192, 3662 and 3707 keV to the well known level scheme of ^{72}Zn. The ground-state β-feeding of ^{72}Zn was derived from comparison of the β-singles and the β-coincident γ-ray spectrum. The β-decays into the 0^+ and 2^+ states indicate a spin of I=1 of the ^{72}Cu ground state. The log ft values do not disagree with an allowed character of these decays. Considering the $1/2^-$ ground state of the N=43 isotones of germanium, selenium and krypton, $I^\pi = 1^+$ is expected for the ground state of ^{72}Cu from the "strong" Nordheim rule. Another comparison can be made with ^{70}Cu [ref. [16]], in which nucleus also neutrons, occupying the $2p_{1/2}$ and the $1g_{9/2}$ shell, couple with the $2p_{3/2}$ proton state to a 1^+ ground state. Comparing these two copper isotopes it is surprising, that the half-life is increased from 5 to 6.6 s, while the Q_β-value is predicted by the mass formulae of ref. [10] to increase by at least 1 MeV, when going from ^{70}Cu to ^{72}Cu.

3.6 THE $^{73}Cu \longrightarrow {}^{73}Zn$ DECAY

In fig. 11 a part of the β-coincident γ-ray spectrum measured at mass 73 is shown. Three groups of γ-lines can be distinguished by their decay properties. Besides known transitions following the β-decay of ^{73}Ga [ref. [6]] another activity was observed, which only slightly decreased in the 7 s measuring-time interval. Since four of these γ-lines are known from a previous study [23] to be transitions in ^{73}Ga, this activity was assigned completely to the decay of ^{73}Zn with a half-life of $T_{1/2}$ = 23.5 s. The resulting decay scheme will be discussed in section 3.7.

In addition to the activities described above we observed a fast decreasing activity in the measured γ-ray spectrum. The 450 keV γ-line determines the half-life value $T_{1/2}$ = 3.9(3) s. All the other transitions given in table 3 show a similar time dependence.

Recently the reaction $^{76}Ge(^{14}C,^{17}O)$ has been applied at the Orsay tandem accelerator to determine the mass of ^{73}Zn and to search for information on excited states in this nucleus; preliminary results [24] of this measurement show a level at 410(50) keV, thus supporting the assignment of the new A=73 activity to ^{73}Cu by its agreement with the strongest γ-transition at 450 keV.

The measured half-life is in rather good agreement with the predicted values for ^{73}Cu (10 and 1.7 s from ref. [18] and ref. [19], respectively), while the predictions for the lower-Z isobaric nuclei ^{73}Co and ^{73}Fe are an order-of-magnitude smaller; furthermore we can exclude these nuclei as emitter of the observed radiation, since estimated cross sections are much smaller than the measured yield. The isotope ^{73}Ni cannot be excluded as a candidate for our observed γ-ray activity on grounds of the half-life prediction of 3 s [ref. [18]], but in the present measurement the extraction of nickel from the ion source was suppressed by a factor of ≳ 10 compared with neighbouring elements (see fig. 1).

3.7 THE $^{73}Zn \longrightarrow {}^{73}Ga$ DECAY

The first identification of ^{73}Zn was reported by Erdal et al. [23], who observed the ß-decay and four ß-delayed γ-transitions. The additional γ-transitions, given in table 4, can be placed in the level scheme of the daughter nucleus ^{73}Ga known from reaction data [25]. The extended decay scheme is given in fig. 12, including a state at 2988 keV, which was added to the previously known levels. The Q_{β}-value of 4.7 MeV used for calculation of log ft values is the endpoint energy of the gross ß-spectrum given in ref. [23]. The intensity of the 218 keV transition has been corrected for internal conversion assuming multipolarity M1.

Vergnes et al. [26] proposed $3/2^-$ or $5/2^-$ as ground-state spin of ^{73}Zn on the basis of reaction data [25] and the γ-ray intensities of Erdal et al. [23]. Particularly the $1/2^-$ assignment expected from the other even-Z N=43 isotones [6] was excluded considering a strong ß-branch into the 496 keV $5/2^-$ state. Our results are not contradictory to the earlier conclusion, although this branch becomes very weak in our work. However, the log ft value of 7.6 disagrees with a spin change of 2.

3.8 THE $^{74}Zn \longrightarrow {}^{74}Ga$ DECAY

In the ß-coincident γ-ray spectrum measured at A=74 we observed known activities from the decays of ^{74}Ga [ref. [6]] and ^{74}Zn. The ß-decay of the latter isotope was first investigated by Erdal et al. [23]. Additionally to the γ-transitions reported by these authors we assigned more γ-lines to ^{74}Zn by time analysis and γγ-coincidences. Our results listed in table 5 together with the results of the previous measurement lead to the decay scheme in fig. 13 including the 3.2 keV isomeric transition in ^{74}Ga, which

was found by van Klinken and Taff [27]. Log ft values were calculated using a Q_{β}-value of 2.45(11) MeV, which was taken from the known mass of ^{74}Ga [ref. [6]] and a recent measurement of the Q-value of the $^{76}Ge(^{14}C,^{16}O)^{74}Zn$ reaction [15]. The present decay scheme extends that given in ref. [27], where the results of Erdal et al. [23] and van Klinken and Taff have been combined and levels at 57, 60, 109 and 250 keV established. The ordering of the 753-142 keV and the 666-119 keV cascades may be reversed, since the respective γ-ray intensities in each cascade are not significantly different; thus no ß-feedings of the intermediate levels are likely to occur. These levels are dashed in fig. 12.

For the lowest lying levels in ^{74}Ga the two possible spin sequences 3^-, (2,3), 0 and 4^-, (3,4), (0,1) with parity change between the second and the third excited state have been derived from the ß-decay of ^{74}Ga, the multipolarity E1 or M1 of the 57 keV, M2 or E3 of the 3.2 keV transition and the non observance of the crossover transition [6,23,27]. The following arguments have been derived from the present experimental results:

a) A comparison of the ^{74}Zn ß-ray intensity (corrected for ß-rays from the decay of ^{74}Ga) with the measured γ-transition intensities shows, that ß-feeding of the ground state and the isomeric state can be neglected. This is in agreement with the earlier assumption of $I^{\pi} = 3^-$ or 4^- for the ground state but contradicts the earlier [27] 1^+ assignment of the 60 keV level.
b) The states at 110, 146, 253, 456 and 895 keV are populated by allowed ß-decays, thus giving $I^{\pi} = 1^+$ for these levels.
c) Assuming no ß-feeding of the 229 keV level we derive an upper limit of $\alpha < 0.3$ for the conversion coefficient of the 119 keV transition and hence the multipolarity E1 or M1. Consequently this transition feeding a 1^+ state at 110 keV restricts the spin and parity of the 229 keV level to be 1^- or $2^{\pm}$. Similar arguments give I=2 for the intermediate 142 keV level.
d) The 53 keV transition is coincident with ß-rays. The experimental coincidence resolving time (t=1 μs) restricts its multipolarity to E1, E2 or M1, using Weisskopf's estimates.

These statements leave only the following spin and parity assignments of the 0, 57 and 60 keV states: i) 3^-, 2, 0 with parity change between second and third level, ii) 3^-, 3^+, 0^- or iii) 4^-, 3^+, (0^-, 1^-), respectively. Thus the earlier assignment for this sequence [27] can be excluded. It should be noted that the possible ordering 3^-, 2^-, 0^+ is realized in the next neighbouring odd-odd gallium isotope ^{72}Ga [ref. [6]].

4. Conclusion

It was the aim of our studies in the rare-earth [2] and in the chromium-germanium region to demonstrate the feasibility of spectroscopic investigations of neutron-rich nuclei outside the classical fission area by means of the multinucleon transfer reaction as production process combined with the on-line mass separation technique. Production yields and separation efficiencies sufficed to get information from $\beta\gamma$- and, in some cases, $\gamma\gamma$-spectroscopic investigations.

The positions of maxima of the isotopic distribution correspond to a ridge connecting ^{56}Mn - ^{75}Ge (see fig. 1). Such a pattern is suggested from the Q_{gg} systematics introduced by Volkov [28], if the shift of 3-4 neutrons towards the stable isotopes caused by neutron evaporation processes is taken into account. A gap in fig. 1 near this line of the highest production yields is explained by the long half-life of ^{59}Fe; samples with masses 60, 64 and 66 were not collected during the present experiment. The identification of activity belonging to nickel isotopes is hindered due to the preference of ground state to ground state β-transitions in the decays of $^{65,67}Ni$ and very likely of ^{68}Ni. Nevertheless, a comparison of the yield of ^{67}Ni, the only nickel isotope identified as reaction product in our work, with yields of observed neighbouring isotopes of copper and cobalt show, that the

extraction of mass-separated nickel sources is suppressed by a chemically selective behaviour of the ion source. This may be effected by formation of NiC in the carbon catcher.

In table 6 the half-lives of the 5 new isotopes identified in this work are compared with theoretical predictions of Takahashi et al. [18] and Klapdor et al. [19]. The calculated half-lives given in ref. [18] are somewhat larger than the experimental ones, whereas the predictions of ref. [19] are smaller except the value of ^{63}Fe. However, the presently available half-life data for neutron-rich manganese-to-copper isotopes do not allow a firm conclusion as to which of the two models is preferable.

The authors would like to thank C. Bruske, K. H. Burkard and W. Hüller for their assistance in operating the on-line separator and the UNILAC crew for their support. One of the authors (K. R.) would like to express his gratitude to GSI Darmstadt for kind hospitality and excellent working conditions.

References

1) Chart of the Nuclides, 5th ed., eds. W. Seelmann-Eggebert, G. Pfennig, H. Münzel and H. Klewe-Nebenius (Gersbach und Sohn Verlag, München 1981)
2) R. Kirchner, O. Klepper, W. Kurcewicz, E. Roeckl, E. F. Zganjar, E. Runte, W.-D. Schmidt-Ott, P. Tidemand-Petersson, N. Kaffrell, P. Peuser and K. Rykaczewski, Nucl. Phys. **A378** (1982) 549
3) D. Guerrau, J. Galin, B. Gatty, X. Tarrago, J. Girard, R. Lucas and C. Ngô, Z. Phys. **A295** (1980) 105
4) R. Kirchner, K. H. Burkhard, W. Hüller and O. Klepper, Nucl. Instr. **186** (1981) 295
5) C. Bruske, K. H. Burkard, W. Hüller, R. Kirchner, O. Klepper and E. Roeckl, Nucl. Instr. **186** (1981) 61
6) Table of Isotopes, 7th ed., eds. C. M. Lederer and V. S. Shirley (Wiley, New York, 1978) and references therein
7) M. Bernas, J. C. Peng, H. Doubre, M. Langevin, M. J. Le Vine, F. Pougheon and P. Roussel, Phys. Rev. **C24** (1981) 756
8) T. S. Bhatia, H. Hafner, R. Haupt, R. Maschuw and G. J. Wagner, Z. Phys. **281** (1977) 65
9) N. B. Gove and M. J. Martin, Nucl. Data Tables **A10** (1971) 206
10) 1975 Mass Predictions, ed. S. Maripuu, Atomic Data and Nucl. Data Tables **17** (1976) 476
11) S. Raman and N. B. Gove, Phys. Rev. **C7** (1973) 1995
12) E. B. Norman, C. N. Davids, M. J. Murphy and R. C. Pardo, Phys. Rev. **7** (1978) 2176
13) A. C. Blair and D. D. Armstrong, Phys. Rev. **151** (1966) 930
14) O. Hansen, M. N. Harakeh, J. V. Maher, L. W. Put, J. C. Vermeulen, Nucl. Phys. **A313** (1979) 95
15) P. Dessagne, Thesis, Orsay 1982, to be published
16) L. M. Taff, B. K. S. Koene and J. van Klinken, Nucl. Phys. **A164** (1971) 565
17) W. L. Reiter, W. H. Breunlich and P. Hille, Nucl. Phys. **A249** (1975)
18) K. Takahashi, M. Yamada and T. Kondoh, Atomic Data and Nucl. Data Tables **12** (1973) 101

19) H. Klapdor, J. Metzinger and T. Oda, to be published, results given in ref.[1]).
20) D. von Ehrenstein and J. P. Schiffer, Phys. Rev. **164** (1967) 1374
21) F. Rösel, H. M. Fries, K. Alder and H. C. Pauli, Atomic Data and Nucl. Data Tables **21** (1978) 113
22) F. R. Hudson and R. N. Glover, Nucl. Phys. **A189** (1972) 264
23) B. R. Erdal, L. Westgaard, J. Żylicz and E. Roeckl, Nucl. Phys. **A194** (1972) 449
24) M. Bernas, P. Dessagne, M. Langevin, J. Payet, F. Pougheon, P. Roussel, W.-D. Schmidt-Ott and P. Tidemand-Petersson, recent result
25) L. P. Ekström and F. Kearns, Nucl. Data Sheets **29** (1980) 1 and references therein
26) M. N. Vergnes, G. Rotbard, E. R. Flynn, D. L. Hanson, S. D. Orbesen, F. Guibault, D. Ardouin and C. Lebrun, Phys. Rev. **C19** (1979) 1276
27) J. van Klinken and L. M. Taff, Phys. Rev. **C9** (1974) 2252
28) V. V. Volkov, Phys. Rep. **44** (1978) 93

Table 1

Energies and relative intensities of γ-rays following the decay of ^{71}Cu

E_γ (keV)	I_γ
128.6(2)	100(7)
184.8(3)	22(6)
197.5(2)	53(6)
489.7(4)	416(34)
520.4(3)	22(9)
586.5(4)	126(9)
595.2(5)	127(8)
668.4(10)	21(8)
674.8(3)	106(10)
1233.6(5)	52(20)
1504.8(5)	42(11)
1791.3(8)	54(16)
2021.7(12)	15(10)

Table 2

Energies, relative intensities and coincidence relations for γ-rays following the decay of ^{72}Cu

E_γ (keV)	I_γ	Coincident γ-lines (keV)	E_γ (keV)	I_γ
534.6(4)	8(2)		1657.7(5)	149(9)
612.2(3)	14(2)		1918.5(8)	15(4)
652.4(3)	1000(31)	846,1005,1251,1540	1993.8(8)	62(5)
797.5(5)	20(3)		2006(1)	32(4)
846.5(3)	114(8)	652	2255(1)	64(8)
858.2(5)	26(3)		2408(2)	48(9)
988.0(5)	17(3)		3008(2)	32(3)
1004.6(3)	177(8)	652	3054(2)	17(4)
1015.7(4)	42(5)		3099(2)	27(4)
1146.4(6)	13(3)		3478(3)	32(4)
1251.4(5)	78(7)	652	3708(4)	17(3)
1516.8(5)	17(3)		3866(3)	70(8)
1540.1(5)	88(7)	652		

Table 3

Energies and relative intensities of γ-rays following the decay of ^{73}Cu

E_γ (keV)	I_γ
199.2(3)	17(2)
306.8(3)	10(2)
449.7(3)	100(5)
502.0(3)	12(2)
674.4(3)	9(3)

Table 4

Energies and relative intensities of γ-rays following the decay of ^{73}Zn

This work		Previous work [23]	
E_γ (keV)	I_γ	E_γ (keV)	I_γ
218.1(2)	1000(31)	216(2)	1000(50)
278.4(4)	16(2)		
415.2(4)	17(2)		
495.6(3)	247(13)	496(2)	260(30)
693.1(3)	63(4)		
910.5(4)	319(13)	911(3)	260(40)
1113.0(4)	49(5)		
1197.3(4)	129(9)	1198(4)	weak
1428.3(5)	15(4)		
1474.3(5)	22(5)		
1612.9(4)	154(9)		
1692.5(6)	36(5)		
1924.7(8)	93(7)		
1979.9(8)	62(6)		
2109(1)	121(9)		
2344(2)	23(4)		
2772(3)	17(3)		
2989(3)	21(3)		

Table 5

Energies, relative intensities, assumed multipolarities and coincidence relations of γ-rays following the decay of ^{74}Zn

This work				Previous work [23]	
E_γ (keV)	I_γ	Multi polarity	Coincident γ-lines (keV)	E_γ (keV)	I_γ
49.4(2)	176(9)	M1	119,144,347,666,785	50.3(5)	71(4)
52.6(2)	51(3)	E1	57,119,144,347	53.1(5)	38(4)
57.1(2)	101(6)	M1	53,89,107,144,196,347,837	57.3(5)	310(23)
85.1(4)	5(1)	M1			
88.8(4)	9(7)	E1	57,107	86.1(5)	14(1)
102.6(5)	6(2)				
107.0(5)	3(1)	M1	57,89		
119.4(3)	14(1)	l=1	49,53	116.7(5)	15(1)
125.7(4)	3(1)				
141.7(5)	35(2)	l=1	753	140.0(5)	142(9)
143.5(4)	114(5)	M1	49,53,57		
149.8(4)	9(1)				
192.5(3)	100(5)	M1		190.4(5)	100(6)
195.6(3)	14(11)	E1	57		
346.7(3)	22(2)		49,53,57	347.3(5)	24(2)
666.2(4)	17(2)		49,119		
752.6(5)	33(1)		142		
785.1(5)	14(2)		49		
837.2(8)	25(2)		57		

Table 6

Measured and predicted half-lives of new isotopes

Isotope	Measured half-life (s) this work	Predicted half-lives (s) ref. [18]	ref. [19]
^{62}Mn	0.88(15)	2	0.77
^{63}Fe	4.9(5)	10	15
^{71}Cu	19.5(16)	35	7.6
^{72}Cu	6.6(1)	7	2.7
^{73}Cu	3.9(3)	10	1.7

Figure captions

Fig. 1. The section of the chart of nuclides investigated in this work. The one-digit numbers indicate the order-of-magnitude of the yields of observed nuclei; 2, for example, stands for saturation intensities between 10^2 and 10^3 atoms/s measured at the focal plane of the mass separator. The values are normalized to a UNILAC beam intensity of 10 particle·nA. For a 1% (arbitrarily assumed) separation efficiency 100 separated atoms/s would correspond to a cross section of 2 mb.

Fig. 2. Part of the γ-ray spectrum for mass 62, measured with a 28% Ge(Li) detector in ß-coincidence. 500 tape-transport cycles were accumulated with 4.2 s collection, 0.2 s transport and 4.2 s counting time each. The average ^{76}Ge beam intensity was 5.9 particle·nA. The insert shows the decay curve of the 876.8 keV γ-rays.

Fig. 3. The decay scheme of ^{62}Mn. Levels observed in few particle transfer reactions are given on the right hand side for comparison [7,8]. The level at 2 MeV has been observed in the (^{14}C,^{16}O) reaction with an accuracy of 60 keV [ref. [7]]. The values in parentheses are absolute transition intensities per 100 ß-decays .

Fig. 4. Part of the ß-coincident γ-ray spectrum measured for A = 63 with a 28% Ge(Li) detector. 33 tape-transport cycles were accumulated with 42 s collection, 0.2 s transport and 42 s counting time each. The beam intensity was 4.6 particle·nA. The decay curve of the 994.8 keV γ-rays is shown in the insert.

Fig. 5. The decay scheme of ^{63}Fe. The numbers given in parentheses are relative transition intensities with I (994.8) = 100. Levels from the $^{64}Ni(t,\alpha)$ reaction [13] are given for comparison.

Fig. 6. The decay curve of ß-rays measured for A = 67 with a 0.5 mm thick plastic scintillator. 26 tape transport cycles were accumulated with 49 s collection, 0.2 s transport and 49 s counting time each. The beam intensity was 6.1 particle·nA.

Fig. 7. Part of the γ-ray spectrum measured at A = 71 with a 15% Ge(Li) detector in ß-coincidence. 61 cycles with 105 s collection and measuring time and 2 s transport time were used for the accumulation of the spectrum. The beam intensity was 6.3 particle·nA. The insert shows the decay curve of the 128.6 keV γ-rays.

Fig. 8. The decay scheme of ^{71}Cu. Intensities of ß-branches and γ-transitions are in relative units (see text). The levels on the right hand side of the scheme were measured in the $^{70}Zn(d,p)$ reaction [20].

Fig. 9. Part of the γ-ray spectrum of ^{72}Cu measured with a 28% Ge(Li) detector in coincidence with ß-rays in a 1.8 h experiment with a 21 s - 0.2 s - 21 s cycle of collection, transport and counting time and a beam intensity of 12.5 particle·nA. Unless otherwise labelled, the γ-lines are assigned to the decay of ^{72}Cu. The insert shows the decay curve of the 652.4 keV γ-rays.

Fig. 10. Decay scheme of ^{72}Cu. Numbers in parentheses are absolute transitions per 1000 ß-decays. The known levels given for comparison were taken from ref. [22]. Dots mark transitions, which were placed on the basis of coincidence measurements.

Fig. 11. Part of the γ-ray spectrum measured at mass 73 in ß-coincidence. 1668 tape transport cycles with 7 s collection, 0.2 s transport and 7 s measuring time were accumulated. The measurement was performed with a 28% Ge(Li) detector and a beam intensity of 12.7 particle·nA.

The insert shows the decay curve of the 449.7 keV γ-rays.

Fig. 12. The decay scheme of ^{73}Zn. The numbers of transitions per 1000 ß-decays are given in parentheses. The intensity of the ß-feeding of the ground state was calculated by comparison of singles ß-rays and ß-coincident γ-rays assuming a 100% branch of the 450 keV transition in the ^{73}Cu decay. A 50% change of this value would only alter the ground-state ß-branch in the ^{73}Zn decay to 88%. Transitions, which have been confirmed by coincidence measurements are marked by dots.

Fig. 13. The decay scheme of ^{74}Zn. Absolute transition intensities are given in parentheses. I (57.1) = 25 is the intensity of the ß-coincident 57 keV transitions and does not include transitions following the decay of the isomeric 60 keV state. Transitions, which are placed on the basis of $\gamma\gamma$-coincidence relations, are marked by dots.

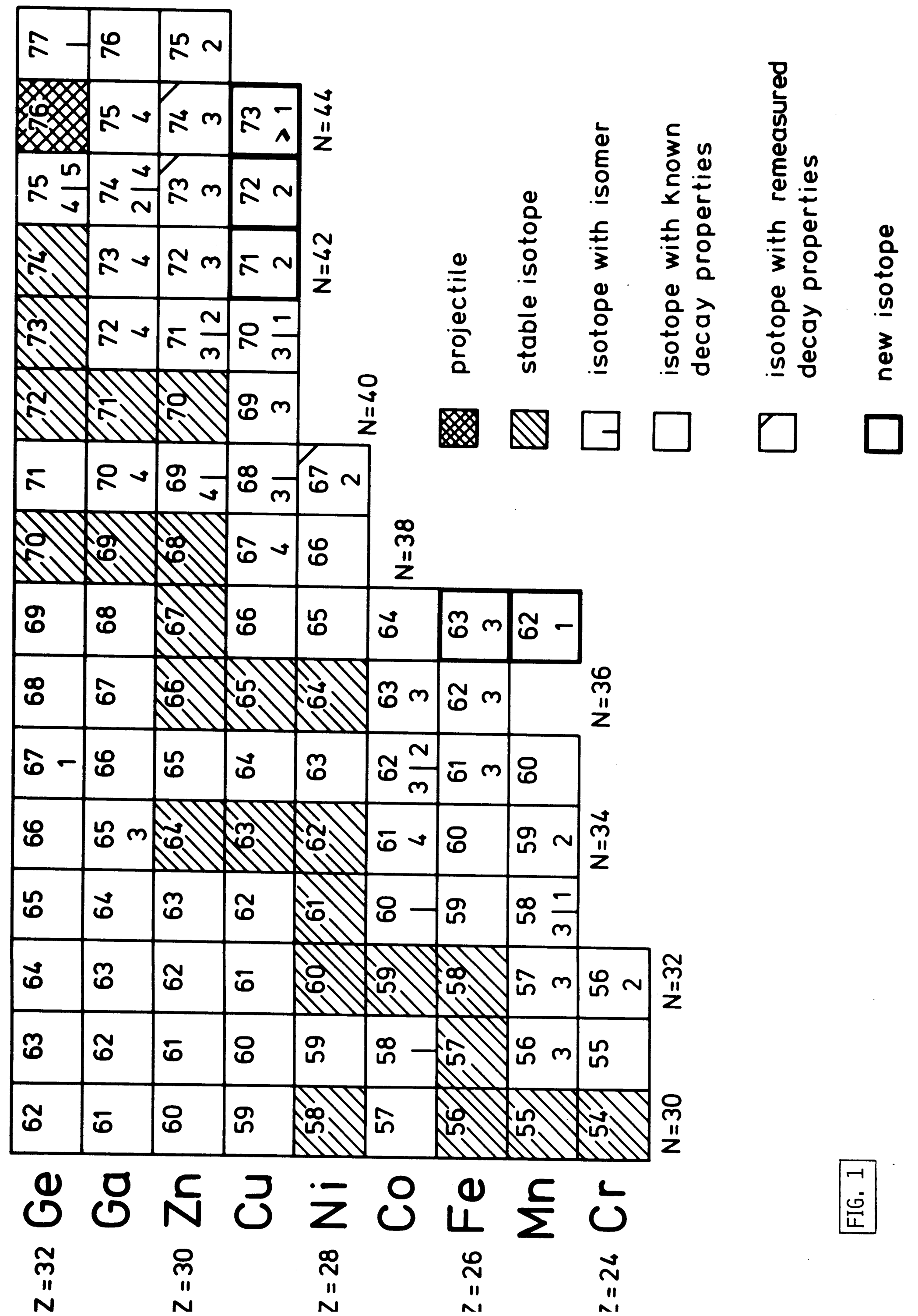

FIG. 1

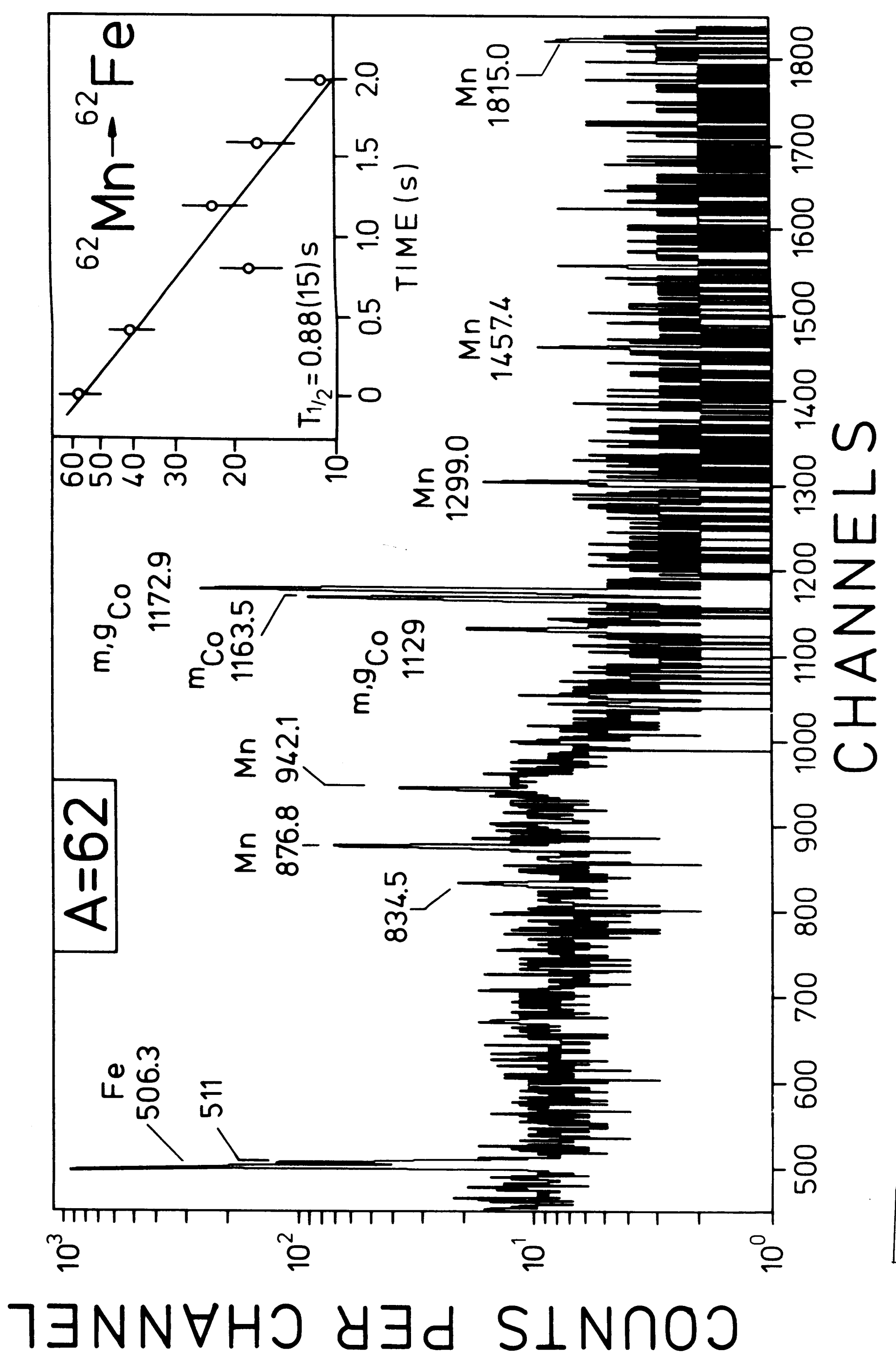

A=62
$^{62}Mn \to ^{62}Fe$
$T_{1/2}$=0.88(15) s
TIME (s)
Fe 506.3
511
Mn 876.8
Mn 942.1
834.5
m,g Co 1172.9
m Co 1163.5
m,g Co 1129
Mn 1299.0
Mn 1457.4
Mn 1815.0
CHANNELS
COUNTS PER CHANNEL

FIG. 2

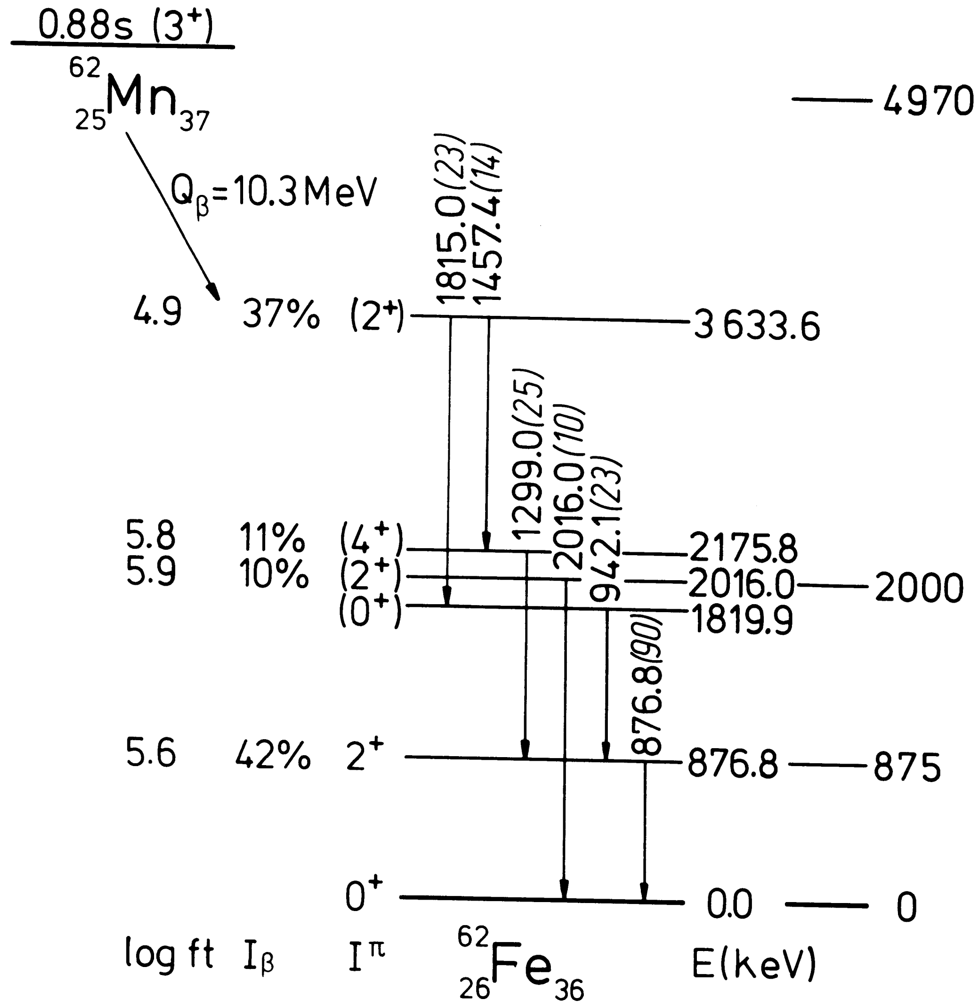

0.88s (3+)
$^{62}_{25}Mn_{37}$
Q_β=10.3 MeV
4.9 37% (2+) 3633.6
5.8 11% (4+) 2175.8
5.9 10% (2+) 2016.0 2000
(0+) 1819.9
5.6 42% 2+ 876.8 875
0+ 0.0 0
1815.0(23)
1457.4(14)
1299.0(25)
2016.0(10)
942.1(23)
876.8(90)
4970
log ft I_β I^π $^{62}_{26}Fe_{36}$ E(keV)

FIG. 3

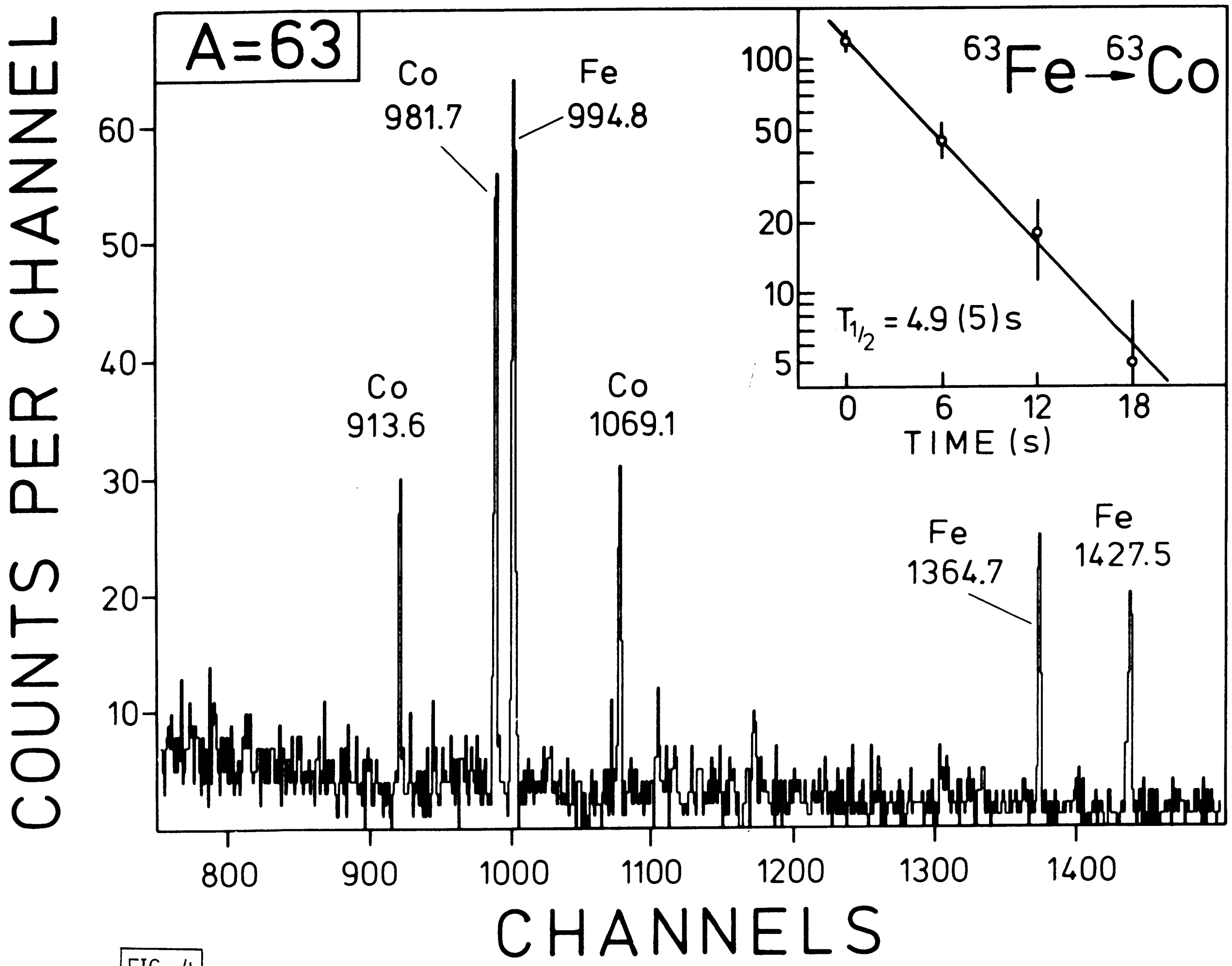
A=63
COUNTS PER CHANNEL
CHANNELS
Co
981.7
Fe
994.8
Co
913.6
Co
1069.1
Fe
1364.7
Fe
1427.5
63Fe→63Co
T1/2 = 4.9 (5) s
TIME (s)

FIG. 4

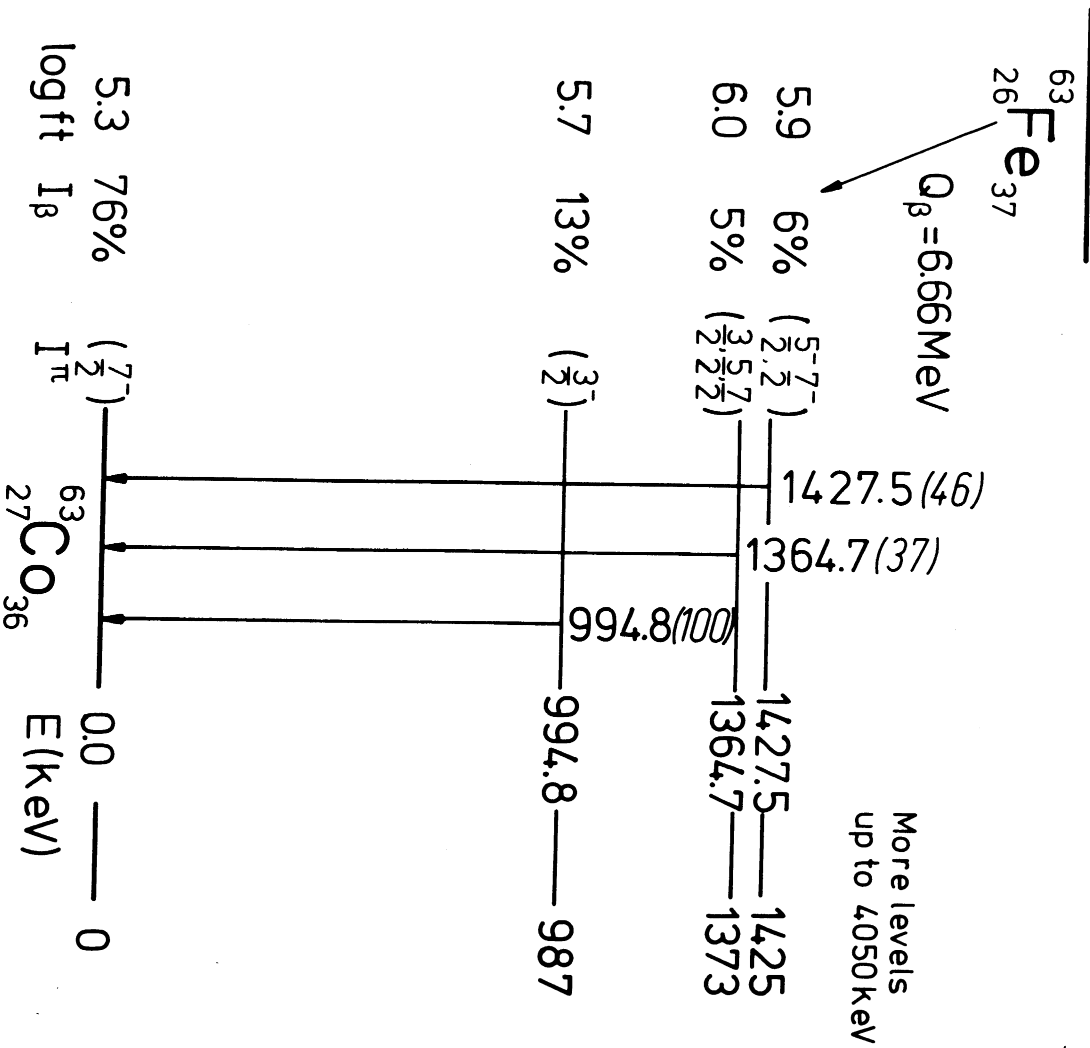
4.9s (5/2-)
63 26 Fe 37
Qβ=6.66MeV
log ft
Iβ
5.9 6%
6.0 5%
5.7 13%
5.3 76%
(5/2-, 7/2-)
(3/2, 5/2, 7/2)
(3/2-)
(7/2-)
Iπ
1427.5 (46)
1364.7 (37)
994.8 (100)
63 27 Co 36
1427.5
1364.7
994.8
0.0
E(keV)
1425
1373
987
0
More levels
up to 4050 keV

FIG. 5

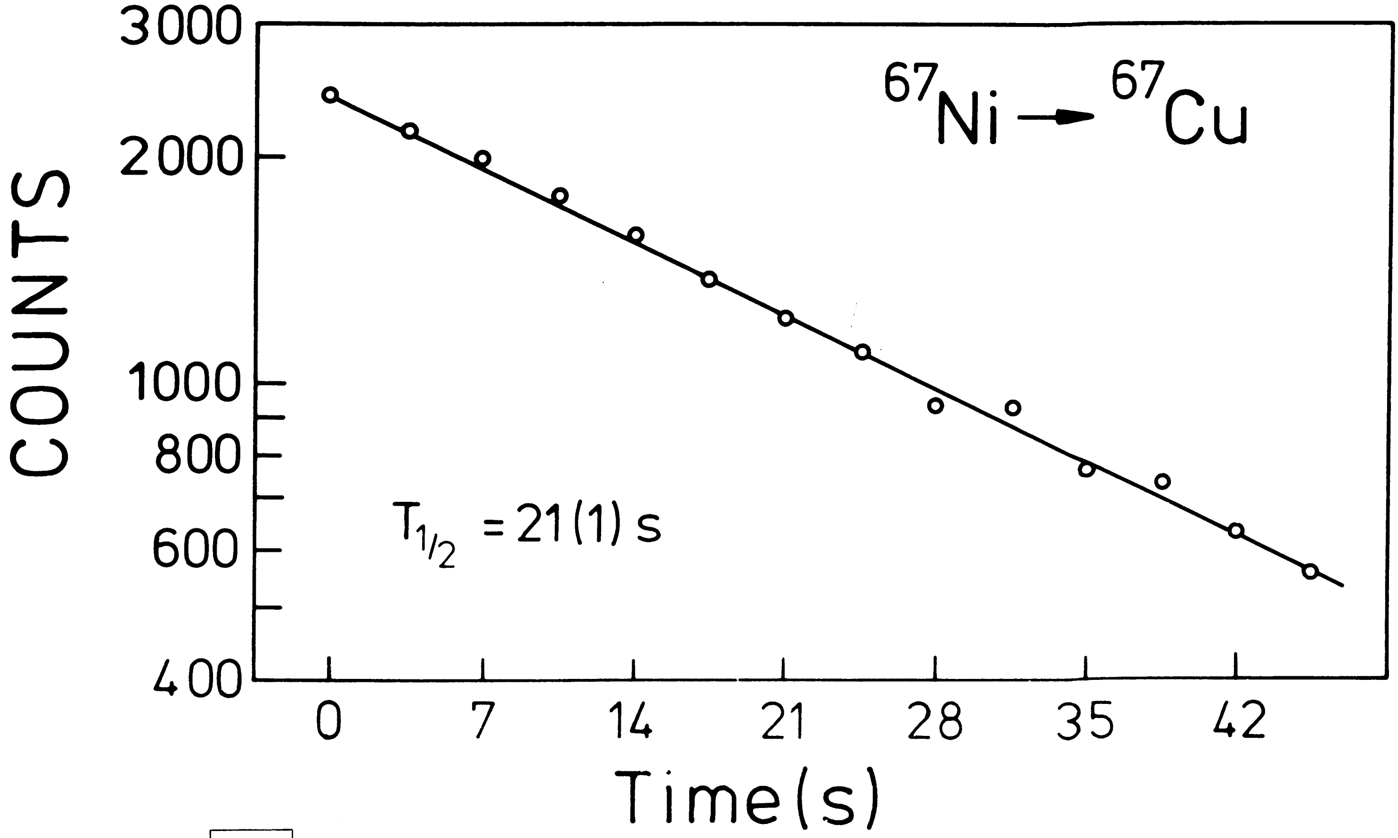

3000
2000
1000
800
600
400
COUNTS
67Ni → 67Cu
T1/2 = 21(1) s
0
7
14
21
28
35
42
Time(s)

FIG. 6

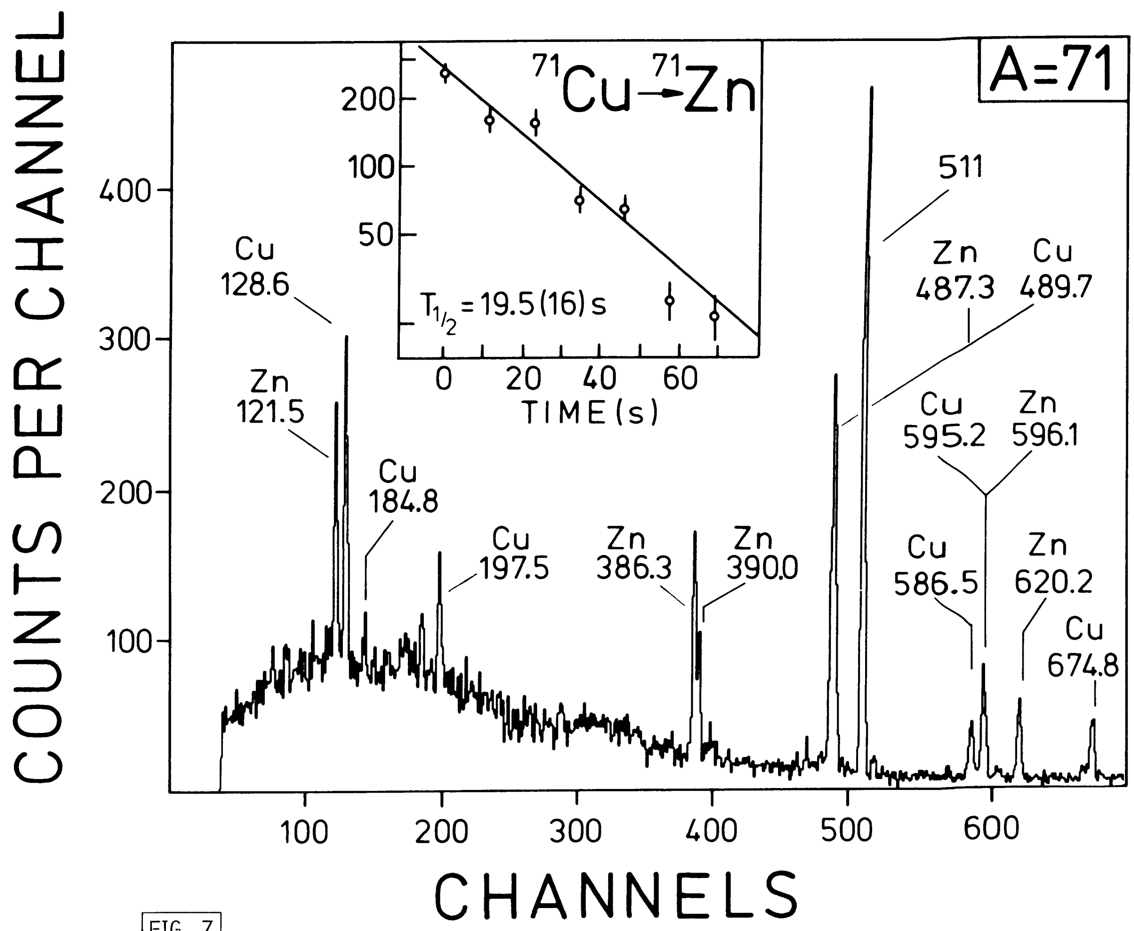

COUNTS PER CHANNEL
400
300
200
100
71Cu→71Zn
200
100
50
T1/2 = 19.5(16) s
0
20
40
60
TIME(s)
A=71
Cu
128.6
Zn
121.5
Cu
184.8
Cu
197.5
Zn
386.3
Zn
390.0
511
Zn
487.3
Cu
489.7
Cu
595.2
Zn
596.1
Cu
586.5
Zn
620.2
Cu
674.8
100
200
300
400
500
600
CHANNELS

FIG. 7

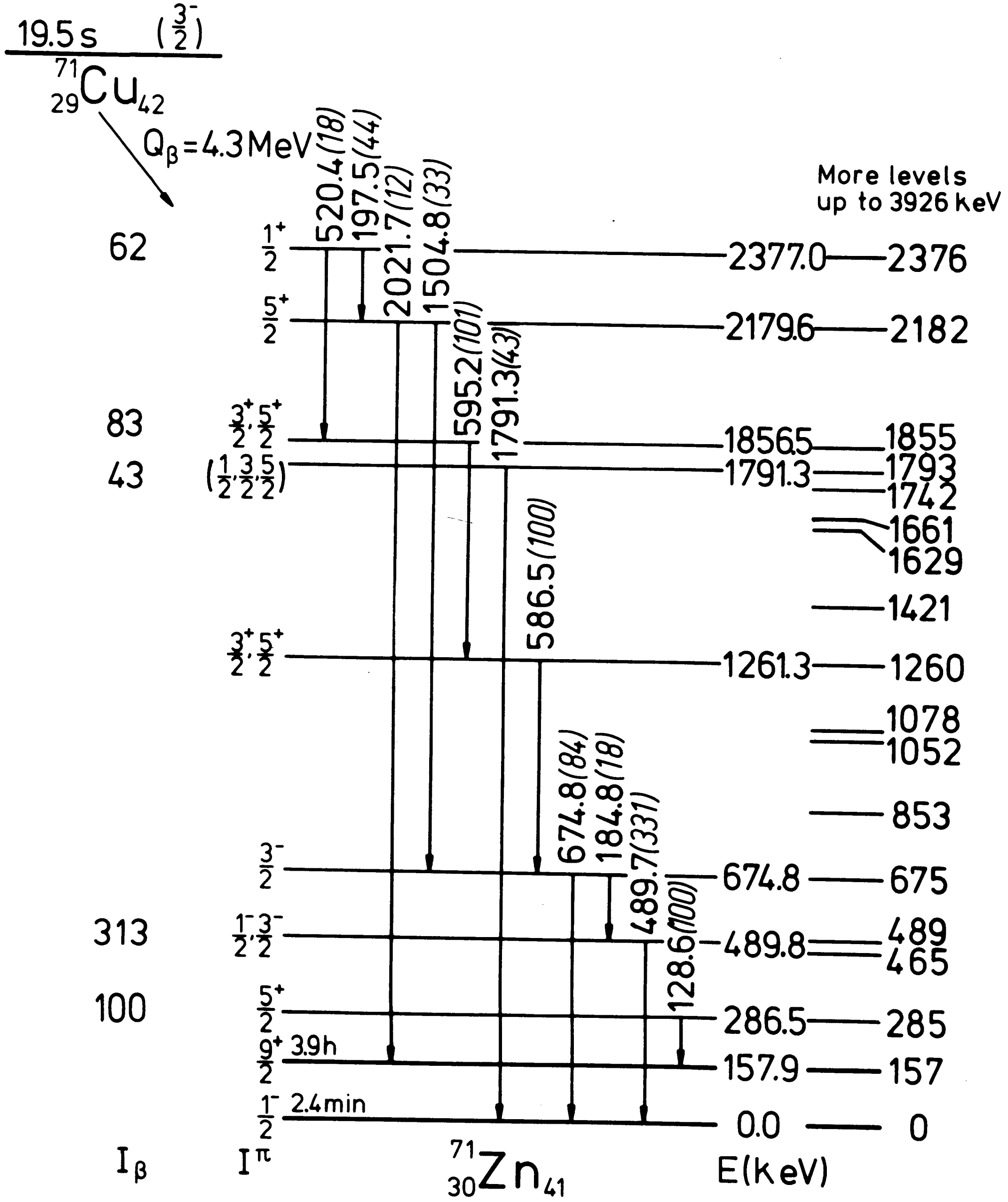
19.5 s (3-/2)
71 29 Cu 42
Qβ=4.3MeV
More levels up to 3926 keV
62
83
43
313
100
520.4(18)
197.5(44)
2021.7(12)
1504.8(33)
595.2(101)
1791.3(43)
586.5(100)
674.8(84)
184.8(18)
489.7(331)
128.6(100)
2377.0
2179.6
1856.5
1791.3
1261.3
674.8
489.8
286.5
157.9
0.0
2376
2182
1855
1793
1742
1661
1629
1421
1260
1078
1052
853
675
489
465
285
157
0
3.9h
2.4min
Iβ
Iπ
71 30 Zn 41
E(keV)

FIG. 8

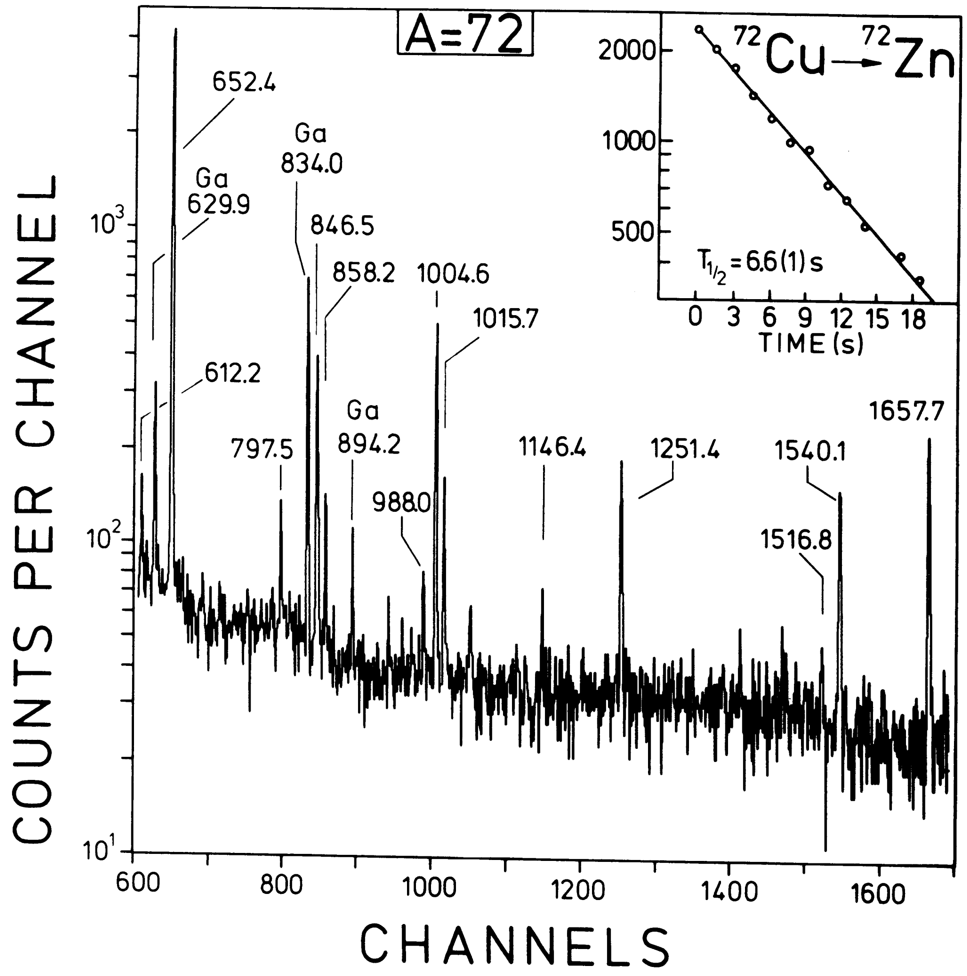
A=72
72Cu → 72Zn
T1/2 = 6.6(1) s
TIME (s)
652.4
Ga 629.9
612.2
Ga 834.0
846.5
858.2
1004.6
1015.7
797.5
Ga 894.2
988.0
1146.4
1251.4
1540.1
1516.8
1657.7
COUNTS PER CHANNEL
CHANNELS

FIG. 9

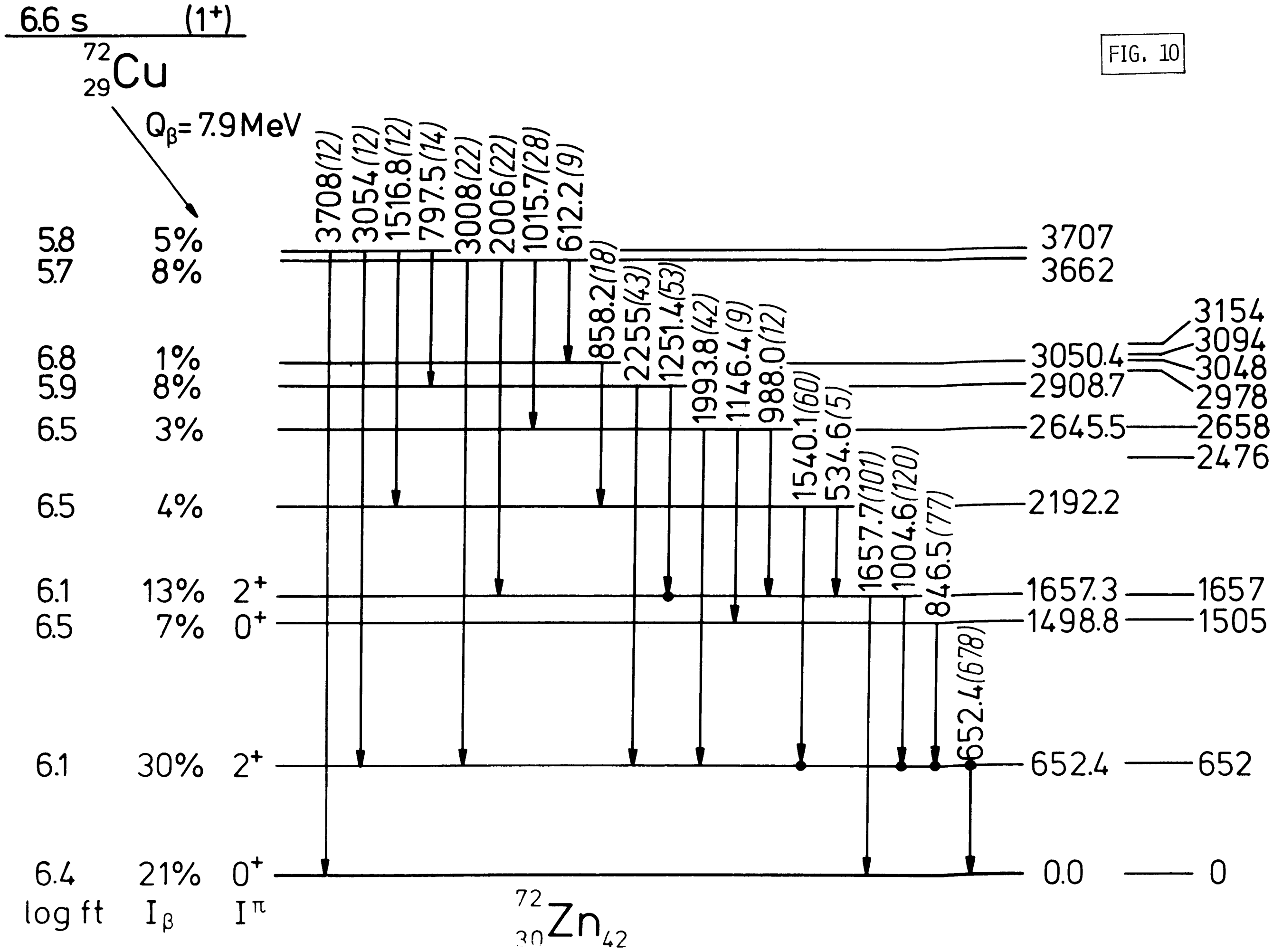

6.6 s (1+)
72 29 Cu
Qβ= 7.9MeV
3708(12)
3054(12)
1516.8(12)
797.5(14)
3008(22)
2006(22)
1015.7(28)
612.2(9)
858.2(18)
2255(43)
1251.4(53)
1993.8(42)
1146.4(9)
988.0(12)
1540.1(60)
534.6(5)
1657.7(101)
1004.6(120)
846.5(77)
652.4(678)
5.8 5% 3707
5.7 8% 3662
6.8 1% 3050.4
5.9 8% 2908.7
6.5 3% 2645.5 2658
2476
6.5 4% 2192.2
6.1 13% 2+ 1657.3 1657
6.5 7% 0+ 1498.8 1505
6.1 30% 2+ 652.4 652
6.4 21% 0+ 0.0 0
3154
3094
3048
2978
log ft Iβ Iπ
72 30 Zn 42

FIG. 10

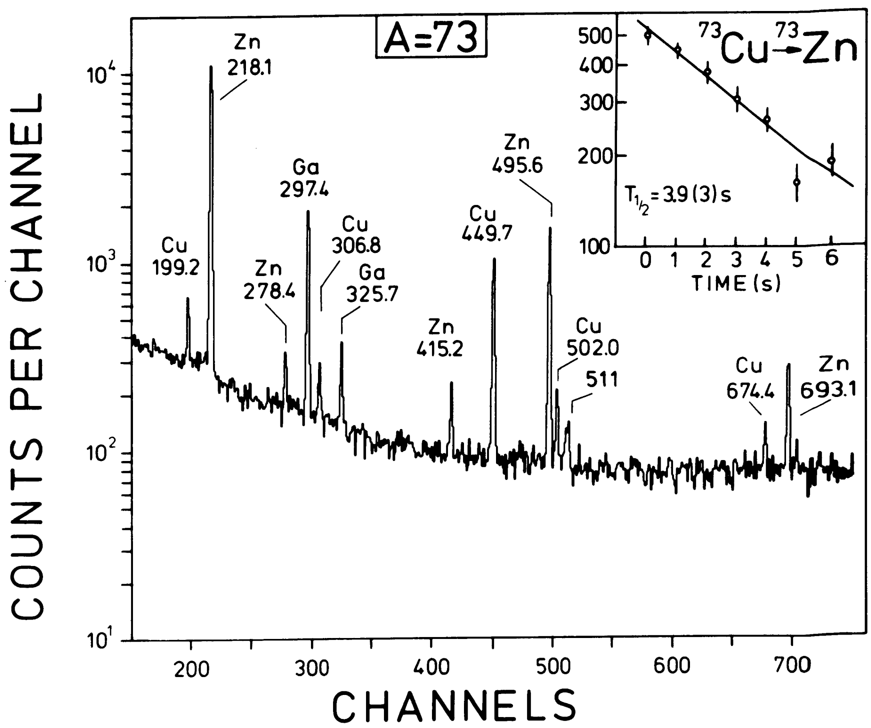

A=73
73Cu→73Zn
T1/2 = 3.9 (3) s
TIME (s)
Zn 218.1
Cu 199.2
Zn 278.4
Ga 297.4
Cu 306.8
Ga 325.7
Zn 415.2
Cu 449.7
Zn 495.6
Cu 502.0
511
Cu 674.4
Zn 693.1
COUNTS PER CHANNEL
CHANNELS

FIG. 11

FIG. 12

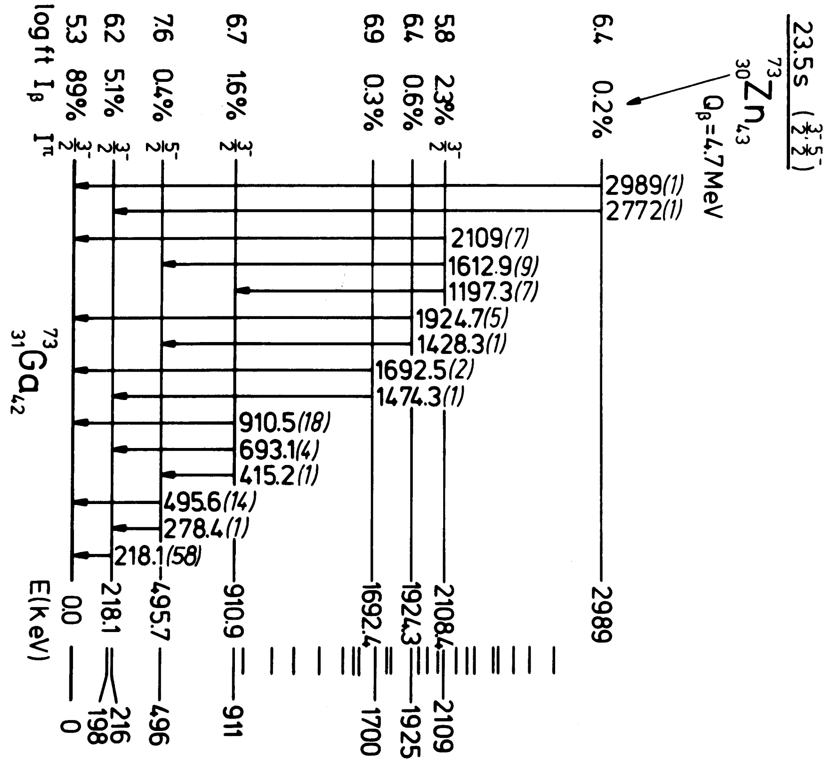
23.5s
73 30 Zn 43
Qβ=4.7MeV
73 31 Ga 42
log ft Iβ Iπ
E(keV)
2989(1)
2772(1)
2109(7)
1612.9(9)
1197.3(7)
1924.7(5)
1428.3(1)
1692.5(2)
1474.3(1)
910.5(18)
693.1(4)
415.2(1)
495.6(14)
278.4(1)
218.1(58)

FIG. 13

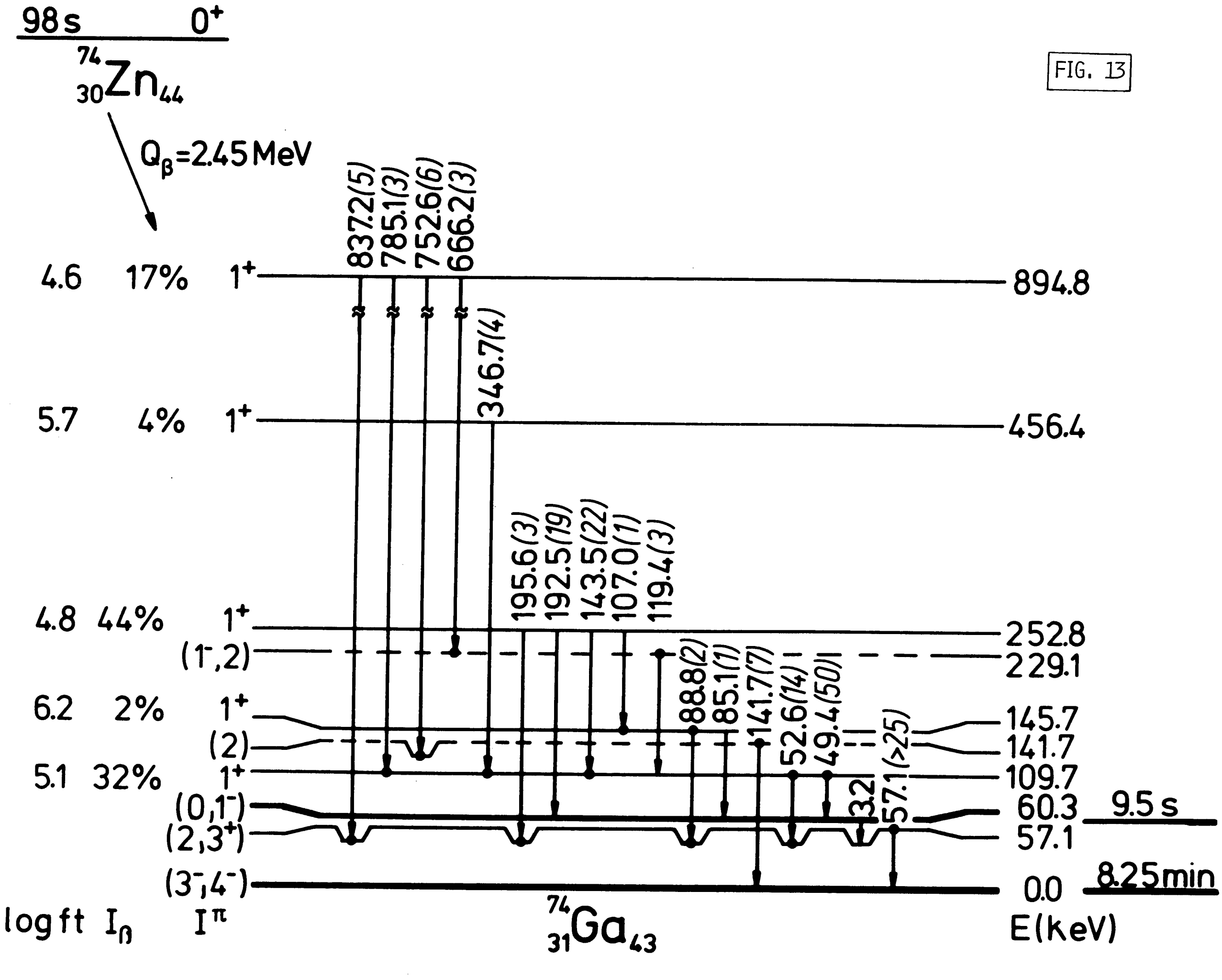
98s 0+
74 30 Zn 44
Qβ=2.45MeV
837.2(5)
785.1(3)
752.6(6)
666.2(3)
346.7(4)
195.6(3)
192.5(19)
143.5(22)
107.0(1)
119.4(3)
88.8(2)
85.1(1)
141.7(7)
52.6(14)
49.4(50)
3.2
57.1(>25)
4.6 17% 1+ 894.8
5.7 4% 1+ 456.4
4.8 44% 1+ 252.8
(1-,2) 229.1
6.2 2% 1+ 145.7
(2) 141.7
5.1 32% 1+ 109.7
(0,1-) 60.3 9.5 s
(2,3+) 57.1
(3-,4-) 0.0 8.25min
log ft Iβ Iπ
74 31 Ga 43
E(keV)